

Deactivation kinetics of Ag/Al₂O₃ catalyst for ethylene epoxidation

G. Boskovic¹, N. Dropka*, D. Wolf, A. Brückner, M. Baerns

Institute for Applied Chemistry Berlin-Adlershof, Richard-Willstätter-Str.12, D-12489 Berlin, Germany

Received 20 January 2004; revised 28 May 2004; accepted 2 June 2004

Available online 2 July 2004

Abstract

Deactivation kinetics of a commercial Ag/Al₂O₃ catalyst was investigated using accelerated deactivation tests in a Berty-type gradientless recycle reactor. Separability of catalytic reaction and deactivation kinetics were established by operation in a “deactivation compensation” mode, keeping temperature and oxygen concentration constant. It was shown that sintering is the main source for deactivation and that kinetics of deactivation can be described by using a general power-law equation with an order of deactivation equal to 1 with respect to the driving force ($a - a_{ss}$), a being the time-dependent activity and a_{ss} the final steady-state activity after an extended period of catalyst operation. The long-time prediction of catalyst behavior suggested that an improved catalyst should work at a lower temperature to avoid sintering.

© 2004 Elsevier Inc. All rights reserved.

Keywords: Deactivation; Kinetics; Ethylene epoxidation; Accelerated deactivation; Deactivation compensation

1. Introduction

Deactivation of catalysts is one of the most investigated problems in industrial catalysis [1] due to its negative impact on both economy and environment. Catalyst improvement is often achieved through identification of sources for its deactivation, with the final goal of preventing deactivation and increasing long-term catalyst activity, selectivity, and stability.

The development of Ag-based catalysts for ethylene epoxidation, which has been the subject of research for many years, is an example of how much effort and time needs to be put into catalyst improvement [2]. Over the years the selectivity of these catalysts improved from about 70% to more than 80% as reported in the patent literature [3]. Nevertheless, stability is still an important issue since these catalysts deactivate under industrial operating conditions. Among several possible mechanisms for deactivation of Ag-based catalyst, sintering of the active metal is broadly accepted as, if not the single, but in any case, the most important one [4–6].

For compensating the loss in catalyst activity under conditions in practice, reaction temperature is usually increased [7]. To prolong the period of high catalyst activity a kinetic model of deactivation predicting the optimal operation mode would be helpful [8]. For this purpose suitable experimental kinetic data of catalyst deactivation must be available. To save time and manpower for long-term catalyst tests, accelerated deactivation on laboratory or bench scale is desirable [1,9,10]; they allow study of the process by broadening the range of reaction conditions [11–13], being an option that is rather restricted in commercial and pilot plant reactors. Furthermore, such accelerated deactivation studies provide deactivated catalyst samples for further *post-mortem* catalyst analysis [1], in a much shorter time span than under regular operation. Benefits from such comprehensive investigation are direct, by means of cost reduction, as well as indirect, through minimization of causes for catalyst deactivation once they have been learned [14].

Although reaction kinetics of Ag-based catalysts for ethylene oxidation was extensively investigated in the past [15–25], rarely any attention has been paid to accelerated deactivation [26,27], and no data were reported related to kinetic modeling of deactivation. It is the goal of the present study to derive deactivation kinetics of a commercial Ag/Al₂O₃ catalyst based on accelerated deactivation tests at the laboratory scale [28], and to validate the obtained model by applying

* Corresponding author. Fax: (49) 30-6392-4454.

E-mail address: dropka@aca-berlin.de (N. Dropka).

¹ On leave from University of Novi Sad, Faculty of Technology, 21000 Novi Sad, Serbia and Montenegro.

the real process parameters over the time scale of commercial application. Eventually, the long-term performance of the reactor can be predicted as previously shown for the methanation of CO [8] by using a suitable reactor model and taking into account the kinetics of both catalytic reaction and deactivation as well as heat and mass-transport processes.

For derivation of deactivation kinetics, the rate equation must be separated in two terms: a term describing the steady-state kinetics of the catalytic reaction at time zero, hence being independent of time, and an activity term, which is by its definition the time-dependent function. If reaction and deactivation kinetics are separable in such a way, the term describing deactivation is merely a function of changing catalyst properties over the time which is, of course, being influenced by reaction conditions [29,30]. That is, only the number of active sites might decrease throughout the experiment [31]. The criterion for separability is the independence of the activity term on temperature and concentration [32]. Thus, by keeping the reactant concentration and the temperature constant, the variation in the rate of reaction is due solely to the deactivation process and can be studied directly.

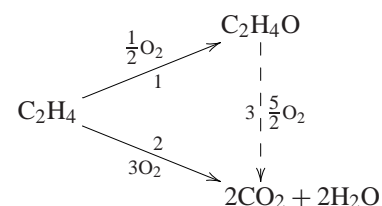
To keep the reactant concentration constant, the conversion must be controlled by decreasing the flow rate and increasing the residence time of the reaction gas mixture, respectively, as the catalyst deactivates [33]. This mode of operation that was the experimental approach applied in this work requires the usage of a gradientless reactor and is known as “deactivation compensation”.

2. Experimental

2.1. Methodology

Previous studies revealed a reduced ability of oxygen adsorption by the partially deactivated commercial catalyst [34]. This might be due to sintering being the main deactivation mechanism of Ag/Al₂O₃ catalysts. Therefore, increasing reaction temperature was one of the parameters chosen for accelerating the deactivation process. Moreover, since it is well known that in many other cases the rate of catalyst sintering is dependent on oxygen concentration [35], oxygen concentration was chosen as an additional variable to cause accelerated deactivation.

The reaction scheme is generally considered to be parallel [25], with two competing reactions involved, i.e., (1) epoxidation and (2) complete combustion:



Depending on the conditions, oxidation of ethylene oxide (3) can also occur, but its rate is generally much slower as com-

pared to those of steps (1) and (2); it is therefore usually neglected. Besides, a zero rate of the ethylene oxide oxidation reaction has been previously reported [36] even in an excess of oxygen. Under our experimental conditions (i.e., low ethylene conversions and no ethylene oxide in the feed), the contribution of the total oxidation of ethylene oxide is expected to be negligible. The fact that ethylene concentration mainly remained constant in the experiments when oxygen was kept constant confirms this presumption.

Since the steady-state kinetics of epoxidation (1) and complete combustion (2) do not depend on the concentration of products [17,25], the condition for the separability of reaction and deactivation kinetics for these steps was fulfilled by keeping the oxygen and consequently ethylene concentration constant during the experiment (in addition to the temperature). Furthermore, assuming a parallel reaction scheme, the rate of formation of ethylene oxide corresponds to the rate of reaction step (1), and the rate of formation of CO₂ corresponds to the rate of reaction step (2). In this case, it is allowed to approximate the activities of the reaction steps (1) and (2) based on the rates of product formation. The global rate of ethylene consumption corresponds to the sum of the rates of reaction steps (1) and (2).

The initial experimental results are rates R_i of C₂H₄O and CO₂ formation,

$$R_i = \frac{F_{\text{tot}}(C_i - C_i^0)}{V_{\text{CAT}}};$$

and C₂H₄ consumption

$$R_{\text{C}_2\text{H}_4} = \frac{F_{\text{tot}}(C_{\text{C}_2\text{H}_4}^0 - C_{\text{C}_2\text{H}_4})}{V_{\text{CAT}}}.$$

The selectivity to C₂H₄O obtained in the gradientless recycle reactor is related to the above rate:

$$S = \frac{R_{\text{EO}}}{R_{\text{EO}} + \frac{1}{2}R_{\text{CO}_2}}.$$

In addition, changes of catalyst activity for C₂H₄ consumption and CO₂ and C₂H₄O formation during the run were calculated as the ratio of rates of formation or consumption of component i at any time t , and at $t = 0$, the latter being defined by the maximal product output during the experiment:

$$a_i = \frac{R_i^t}{R_i^{t=0}}.$$

2.2. Experimental procedure

Accelerated deactivation tests were performed with an Raschig ring-type Ag-based catalyst close to commercial version, in a computer-controlled internally mixed flow reactor. The experiments were carried out under a set of initial conditions shown in Table 1, which were discussed elsewhere [28]. The chosen variables, i.e., temperature and O₂ concentration at maximal catalyst activity [28], were kept

Table 1
Operating parameters in accelerated deactivation experiments

	Operating parameter	Range
Variables	T (K)	533–553
	$C_{O_2, in}^a$ (vol%)	1.5–7.5
Constant parameters	$C_{C_2H_4, in}$ (vol%)	25
	$C_{CO_2, in}$ (vol%)	5.5
	Chlorine (as ethyl chloride) (ppm)	1.8
	P (bar)	20
	Space velocity $_{t=0}$ (h^{-1})	25,000

In every experiment N_2 was used as balance to 100 vol%.

^a O_2 concentrations at inlet; results in the text are referred to O_2 concentrations at zero deactivation time, i.e., at maximal catalyst activity.

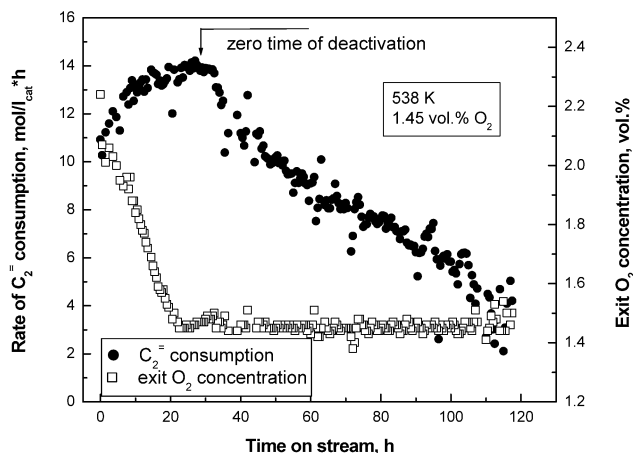


Fig. 1. Path of a typical deactivation experiment in the form of rate of ethylene consumption as a function of total time on stream (total time on stream includes activation time for reaching maximal activity).

constant throughout a single experiment. In principle, deactivation compensation by constant reactant concentration can be approached either by changing the flow of a single component responsible for deactivation or by changing the total inlet flow (the concept used in this study), resulting in constant conversion [37]. In a typical experiment, the initial space velocity was as high as $25,000 h^{-1}$, and then it was gradually decreased during time on stream with a rate depending on how fast catalyst deactivation had progressed.

2.3. Experimental results and discussions

2.3.1. Influence of temperature and O_2 concentration on deactivation rate

The initial catalyst activity was usually established after several hours upon first contact of the catalyst with the reaction gas mixture during which the rates of consumption of ethylene increased (Fig. 1). The length of the period depended on the severity of the applied deactivation conditions. In this period, the combined effect of catalyst activation and initial mixing of gases was over, giving a stable operation further on. The maximum rate of ethylene consumption coincides with the minimum of O_2 concentration [28]. At that point the catalyst started to deactivate, which was

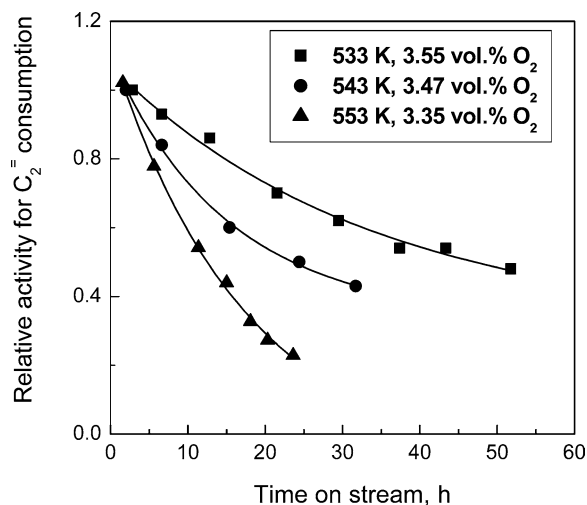


Fig. 2. Dependence of relative catalyst activity for ethylene consumption $a_{C_2}^t = R_{C_2}^t / R_{C_2}^0$ on time on stream at high O_2 concentration.

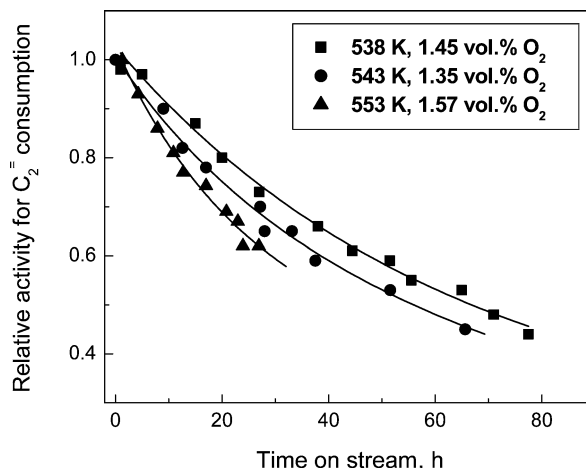


Fig. 3. Dependence of relative catalyst activity for ethylene consumption $a_{C_2}^t = R_{C_2}^t / R_{C_2}^0$ on time on stream at low O_2 concentration.

observed as both ethylene oxide and CO_2 concentration decreased, and O_2 concentration increased. This situation was taken as time “zero” of deactivation and it accounts for initial relative activity and initial selectivity. Starting at time zero, the action of deactivation compensation was carried out by means of keeping the corresponding O_2 concentration in the reactor constant. Therefore, every experiment corresponds to an oxygen concentration in the reactor obtained at zero time of deactivation which was between 0.87 and 4.80 vol% for individual runs, and this concentration was kept constant by a gradual increase of contact time [28].

The temperature at which the reaction occurs is crucial for the deactivation rate (see Fig. 2). A similar behavior can be seen at low oxygen concentration, presented in Fig. 3, with the temperature effect being not so marked, however. By comparing Figs. 2 and 3 it is obvious that at high oxygen concentrations, the rate of deactivation is higher.

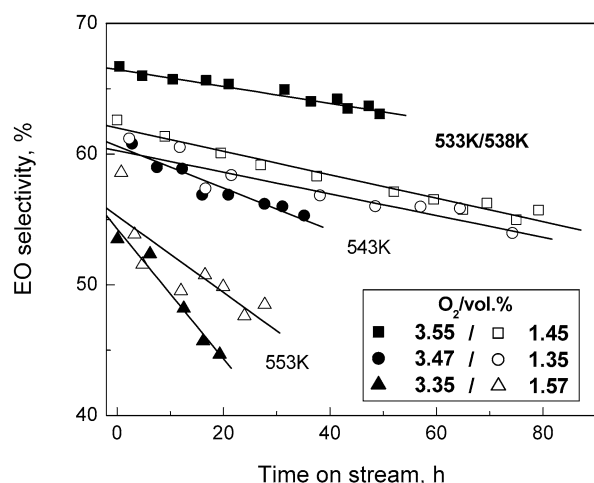


Fig. 4. Dependence of an ethylene oxide selectivity on time on stream at 533/538 K (□), 543 K (○), and 553 K (△) (numbers in the right-hand box represent O₂ concentrations within the reactor, in vol%).

Values of initial selectivity and profiles of temporal selectivity changes with time on stream are also dependent on reaction temperature and oxygen concentration as well: the higher the temperature the lower the initial selectivity and the steeper the selectivity decay over time, as presented in Fig. 4. However, the influence of oxygen concentration on selectivity changes with temperature: at 543 and 553 K, higher concentrations slightly decrease the initial selectivity and increase the rate of selectivity decay. At the lowest temperature applied (533 K), the effect is the opposite; the initial selectivity is higher for the higher oxygen concentration. The decay of selectivity over time is nearly parallel for both values of the oxygen concentration (Fig. 4). The slightly higher temperature performed with lower O₂ concentration, i.e., 538 K vs 533 K, may introduce some doubt in the previous conclusion. However, another set of experiments performed with different O₂ concentration at constant temperature of 533 K (Fig. 6) support the positive impact of higher O₂ concentration on initial selectivity at low reaction temperature.

An interesting feature of relative catalyst activity (Fig. 5) and selectivity (Fig. 6) can be seen when the concentration of oxygen is gradually changed: The relative activity decay of the catalyst increases, in principle, with oxygen concentration. Selectivity, however, shows a more complex behavior. At 553 K selectivity decreases with increasing oxygen concentration and the selectivity drop becomes steeper (Fig. 6). At 533 K, however, the trend is opposite: the selectivity is highest for the highest O₂ concentration and the selectivity drop is not influenced by the O₂ concentration level (Fig. 6). This could stand for a possible “healing” effect of higher oxygen concentrations due to burning of carbon species, which might accumulate over a long time of catalyst exploitation. A different dependence of selectivity on O₂ concentration at different temperatures may be understood as the result of a complex contribution of two deactivation mechanisms, i.e., sintering and coking. At 553 K sintering

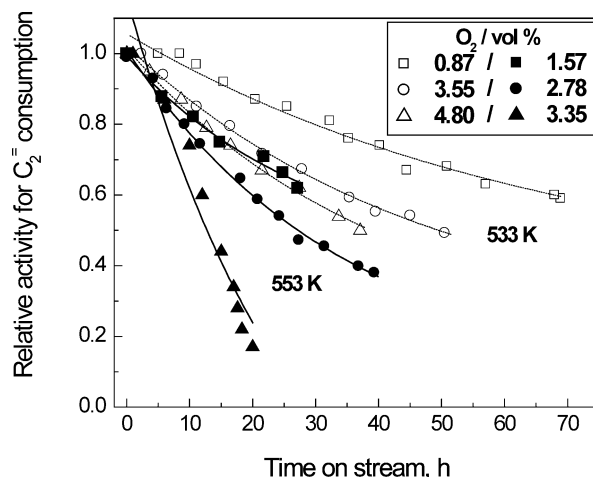


Fig. 5. Dependence of relative catalyst activity of C₂H₄ on O₂ concentration at 533 K (blank symbols), and 553 K (filled symbols) (numbers in the right-hand box represent applied O₂ concentrations, in vol%).

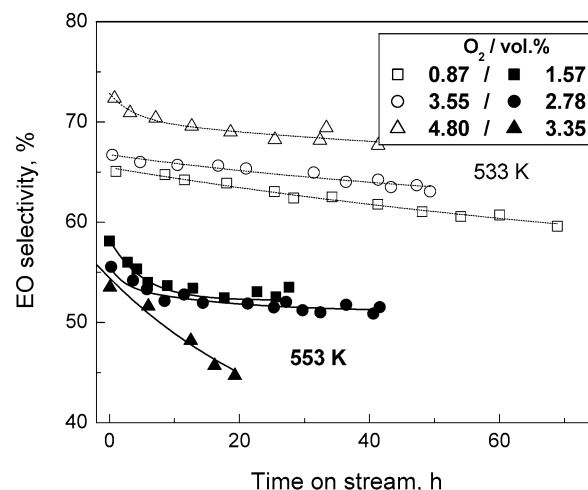


Fig. 6. Dependence of ethylene oxide selectivity on O₂ concentration at 533 K (blank symbols), and 553 K (filled symbols) (numbers in the right-hand box represent applied O₂ concentrations, in vol%).

is very much dominant over coking, and therefore cannot be compensated by a positive impact of higher O₂ concentration on coke burning. Such self-cleaning ability of an Ag-based catalyst by means of transformation of intermediate surface deposits from ethylene to CO₂, has been reported in the literature for cases of oxygen-rich feed compositions [17,20].

The decrease in EO selectivity with time on stream is a general feature noted for the whole range of temperatures and oxygen concentrations applied. The reason for different changes of reaction rates of the formation of ethylene oxide and CO₂ may be due to changes in the proportion of different active sites for selective and total oxidation during reactor operation. From Fig. 7 it becomes obvious that the selectivity drop results from the drop in ethylene oxide concentration while CO₂ concentration stays constant. Data from the literature suggest that ethylene oxidation might be

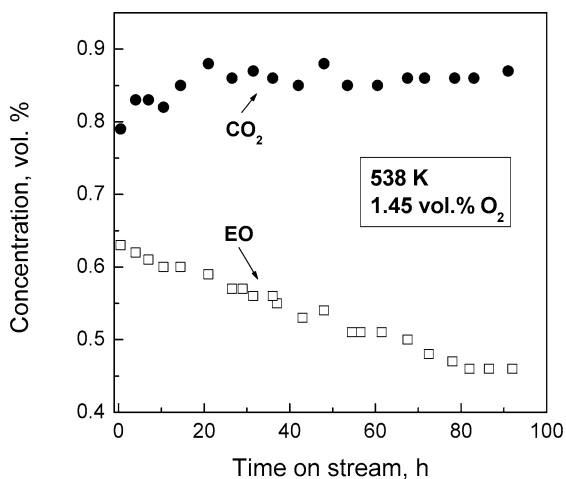


Fig. 7. Temporal concentration profiles of products of a typical accelerated deactivation experiment.

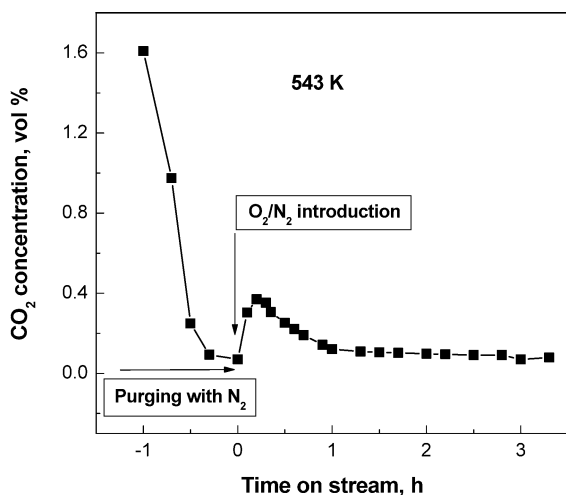


Fig. 8. Evolution of CO₂ from the catalyst previously exposed to 543 K and 1.35 vol% O₂ for 80 h; prior to introducing 2 vol% O₂/N₂ flow, the catalyst was purged with pure N₂ flow for 1.5 h.

a structure-sensitive reaction [4,5]. If concurrent reactions of selective and total oxidation occur on catalyst sites with different coordination numbers, the relative fraction of these sites may change due to sintering. Another explanation for a selectivity change could be coke deposition by ethylene decomposition, or surface carbonate formation from CO₂. An indication for the presence of deposits is the evolution of CO₂ in a flow of O₂ (2 vol%)/N₂ mixture, from the surface of a deactivated catalyst (Fig. 8); in this experiment the catalyst had previously been purged with pure N₂ until no traces of CO₂ were observed anymore. Integration of the area below the curve in Fig. 8 results in ca. 550 μmol CO₂ as a result of the treatment of the spent catalyst by O₂/N₂ mixture over 3 h.

Some authors claim inhibition of ethylene oxide formation by surface carbon species, which can be formed either by CO₂ decomposition [23,38], or by direct oxidation of ethylene [39]. Carbon deposition on the catalyst surface could

itself be a structure-sensitive reaction [40], building up the coke preferentially on specifically coordinated Ag sites, and consequently influencing the selectivity by inhibiting ethylene oxide formation.

3. Kinetics of deactivation

3.1. Methodology

A general attempt in the elucidation of deactivation kinetics from an accelerated deactivation test is to find an equation that describes the catalyst activity decline as a function of time. On this basis the catalyst lifetime can be predicted; if the kinetics of the catalytic reaction are also known, a temporal activity profile within the reactor and its overall performance can be simulated. The overall kinetics may be described by

$$R_i = f_1(T, p_j) \cdot f_2[a_i(t, T, p_k)]. \quad (1)$$

The function f_1 represents the kinetic term of the catalytic reaction, and f_2 the deactivation term, respectively; species i , j , and k can be ethylene, ethylene oxide, oxygen, and CO₂. The industrial problem of a deactivation of commercial Ag-based catalysts for ethylene oxidation is essentially a selectivity decrease [2]. It is necessary to determine the catalyst activity term in Eq. (1) as a function of both ethylene oxide and CO₂ rates of formation. Then, on condition that the intrinsic kinetics for these products are known, it is possible to calculate the time to reach an allowable minimal process selectivity [41]. However, since the elucidation of the reaction kinetics of the Ag-based commercial catalyst examined was not the aim of the present investigation, the effort was focused on modeling the kinetics of deactivation only to predict the decay in the output of ethylene oxide and CO₂ as well as the decrease in ethylene conversion over the time of catalyst exploitation under specific conditions as realized in a controlled gradientless recycle reactor. Change of catalyst activity with time on stream is described by an equation originally derived by Levenspiel [29], but later modified by introducing the term of steady-state activity, a_{ss} , reached at infinite time [42]:

$$-\frac{da}{dt} = k_d \cdot p_{O_2}^\alpha \cdot (a - a_{ss})^d. \quad (2)$$

The above general power-law equation (GPLe) stands for the fact usually observed in industrial catalysis, that activity does not drop to zero, but to a steady-state value [35,42]. The goal is to express temporal activity as a function of the various parameters of Eq. (2), i.e., k_d , α , a_{ss} , and d . The analytical solution of Eq. (2) for $d \neq 1$ is given as

$$(a - a_{ss})^{1-d} - (1 - a_{ss})^{1-d} = (d - 1) \cdot k_d \cdot p_{O_2}^\alpha \cdot t. \quad (3)$$

The integrated form of Eq. (2) for the special case of $d = 1$ is given by

$$a = a_{ss} + (1 - a_{ss}) \cdot \exp\left(-k_d^0 \exp\left(-\frac{E_A}{RT}\right) p_{O_2}^\alpha t\right). \quad (4)$$

Table 2
Kinetic parameters for deactivation model for CO₂, C₂H₄, and C₂H₄O

	C ₂ H ₄ O	CO ₂	C ₂ H ₄
$k_d^0 \times 10^{-5}$ (h ⁻¹ MPa ^{-α})	1.4 ± 0.6	73.5 ± 45.9	0.28 ± 0.12
E_A (kJ/mol)	63.0	77.0	55.2 ^a
α (-)	0.49 ± 0.1	0.81 ± 0.15	0.59 ± 0.10
a_{ss} (-)	0.24 ± 0.1	0.30 ± 0.15	0.19 ± 0.14

^a E_{app} .

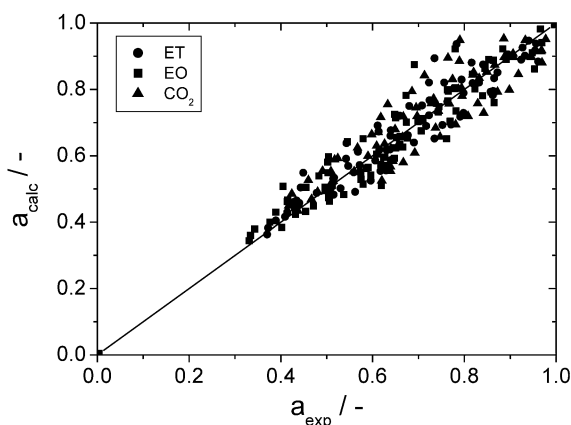


Fig. 9. Parity plot for activity of ethylene, ethylene oxide and CO₂ experimental versus calculated value according to Eq. (4).

The values of d , k_d^0 , E_A (in case of ethylene E_{app}), α and a_{ss} were obtained solving Eq. (3) numerically by nonlinear regression method (Athena Visual Workbench 8.3).

3.2. Modeling results and discussions

The best fit of all experimental data to Eq. (4) was obtained for deactivation rate order d with respect to $(a - a_{ss})$ for a value close to 1. The ability of the GPLe to describe the kinetics of sintering of different catalysts by simply applying deactivation rate order as 1 or 2 was reported in the literature [35,42,43]. For d equal 1, the theory suggests [37] that it is a case of parallel deactivation with no pore-diffusion resistance to the reactant responsible for deactivation (oxygen in this study). Setting d equal to 1, values of k_d^0 , E_{app} , α , and a_{ss} were calculated again numerically for the integrated Eq. (4). The dependence of EO selectivity on time on stream at the highest temperature of 553 K and oxygen concentration 3.35% could not be included in the model when fitting the data simultaneously. It is anticipated that the mechanism of deactivation changes significantly at higher temperatures; this issue needs additional study for elucidating the underlying phenomena. In the case of ethylene oxide formation, the order of 0.5 with respect to oxygen suggests dissociative adsorption of oxygen. Results are shown in Table 2. The parity plot, presented in Fig. 9 shows a satisfactory agreement between experimentally obtained and calculated catalyst activity values for all three components. Accordingly, good agreement between experimental (symbols) and calculated (lines) values was obtained for different temperatures and oxygen concentrations (Fig. 10). Different values of steady-state activities for ethylene oxide and CO₂ confirm the fact that selectivity is decreasing with a time reaching fi-

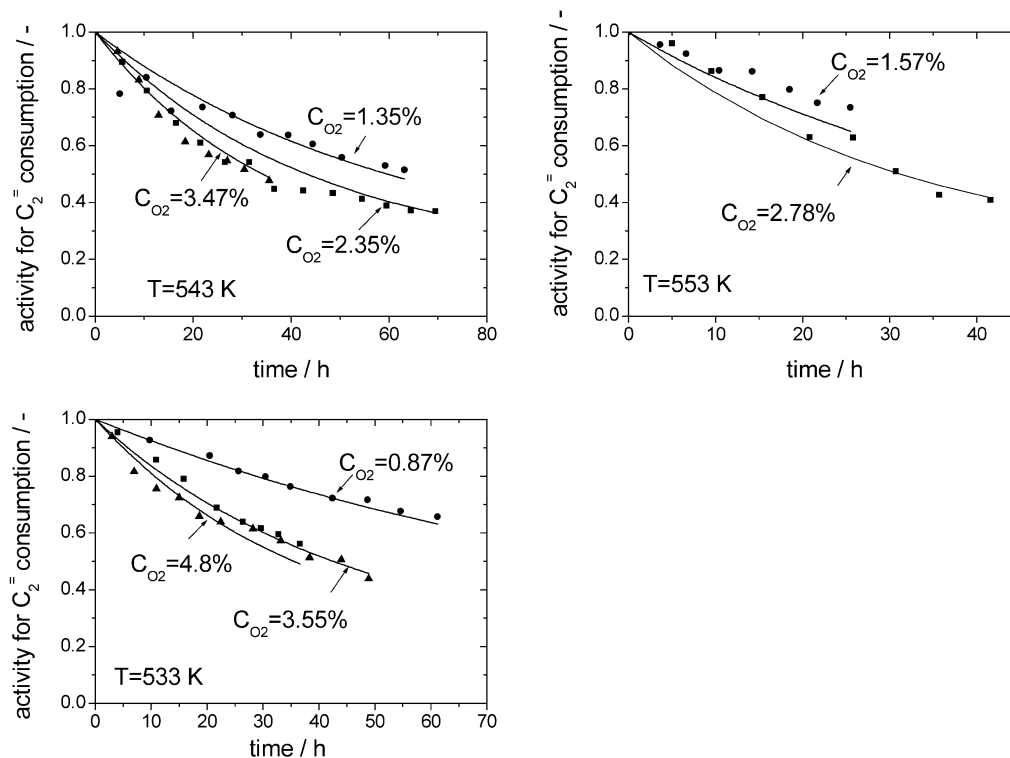


Fig. 10. Model validity test: activity of ethylene versus time on stream for different temperatures and oxygen concentrations (lines: simulation, points: experimental).

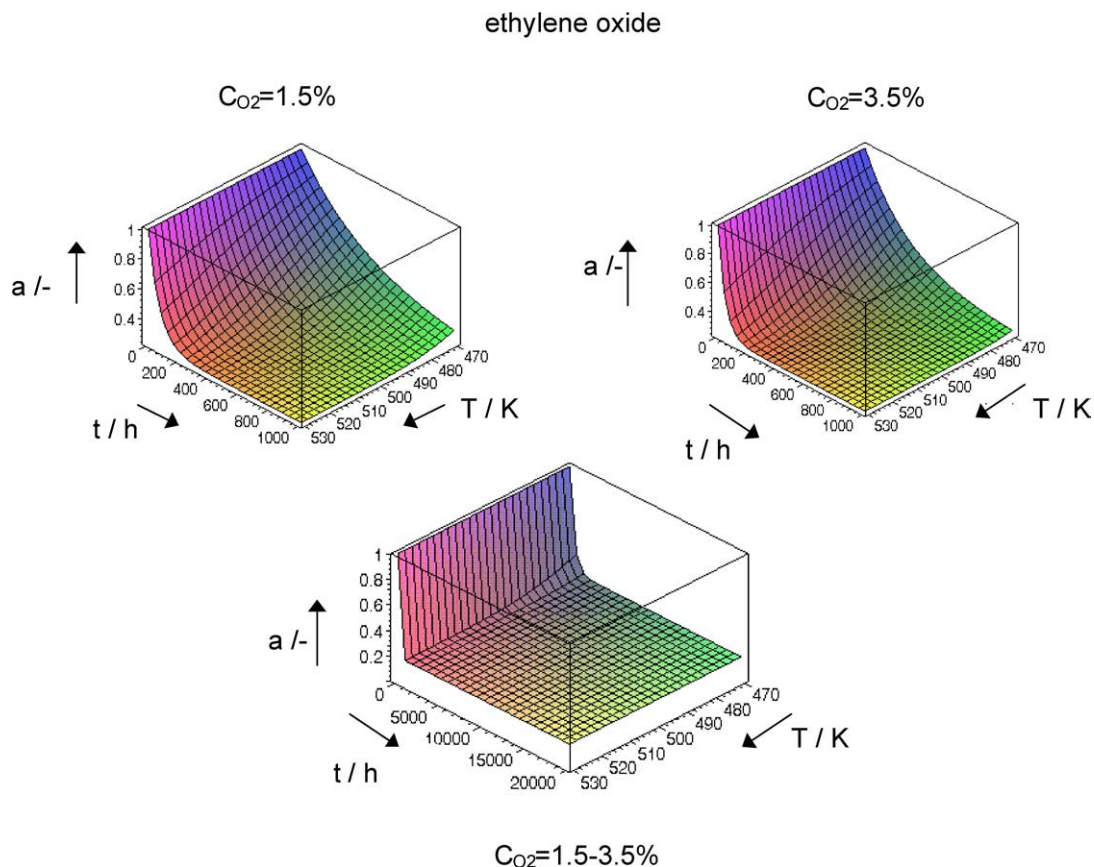


Fig. 11. Long-time prediction of catalyst activity of C₂H₄O for different concentrations of oxygen for operation of a gradientless reactor, based on the kinetic model given by Eq. (4).

nally:

$$\begin{aligned}
 S_{ss,EO} &= \frac{1}{1 + \frac{1}{2}(R_{CO_2}/R_{EO})_{ss}} \\
 &= \frac{1}{1 + \frac{1}{2}(R_{CO_2}^0 a_{ss,CO_2}/R_{EO}^0 a_{ss,EO})} \\
 &= \frac{1}{1 + \frac{1}{2}(R_{CO_2}^0/R_{EO}^0) \times 1.25}.
 \end{aligned}$$

In order to study the influence of temperature and oxygen concentration on the steady-state activity, its value was determined by a nonlinear regression method for each combination of experimental conditions separately. The resulting values of steady-state activities had too wide confidence intervals and therefore the influence of temperature and oxygen concentration could not be estimated with any statistical significance.

Simulations of the catalyst activity for ethylene and ethylene oxide over a period of 20,000 h on stream carried out for both low and high O₂ concentrations are shown in Figs. 11 and 12. The activities drop to the steady-state value in less than 1000 h; this time span may be different from industrial practice since there is a temporal concentration and activity profile in the fixed-bed reactor. The deactivation kinetics derived can be used for simulating the performance of the

plug-flow reactor [8]. The influence of temperature and oxygen concentration is very important in the initial stage before steady state is reached, during which they determine the rate of deactivation. Later, on a long-term basis, their influence becomes negligible.

4. Conclusions

In the applied range of conditions, deactivation of a commercial Ag/Al₂O₃ catalyst was successfully described by using the general power-law equation with an order of 1 with respect to the driving force ($a - a_{ss}$). Since deactivation kinetics suggests only a weak influence of oxygen concentration related to deactivation, there is no large difference in deactivation rates in simulated long-time commercial runs at different O₂ concentrations.

Values of initial and temporal selectivity depend on reaction temperature: the higher the temperature the lower the initial selectivity and the steeper the selectivity decay over time. The influence of oxygen concentration on both selectivities changes with temperature: at higher temperatures, higher concentrations of oxygen slightly decrease the initial selectivity and increase the rate of selectivity decay; at the lower temperature, the effect is the opposite.

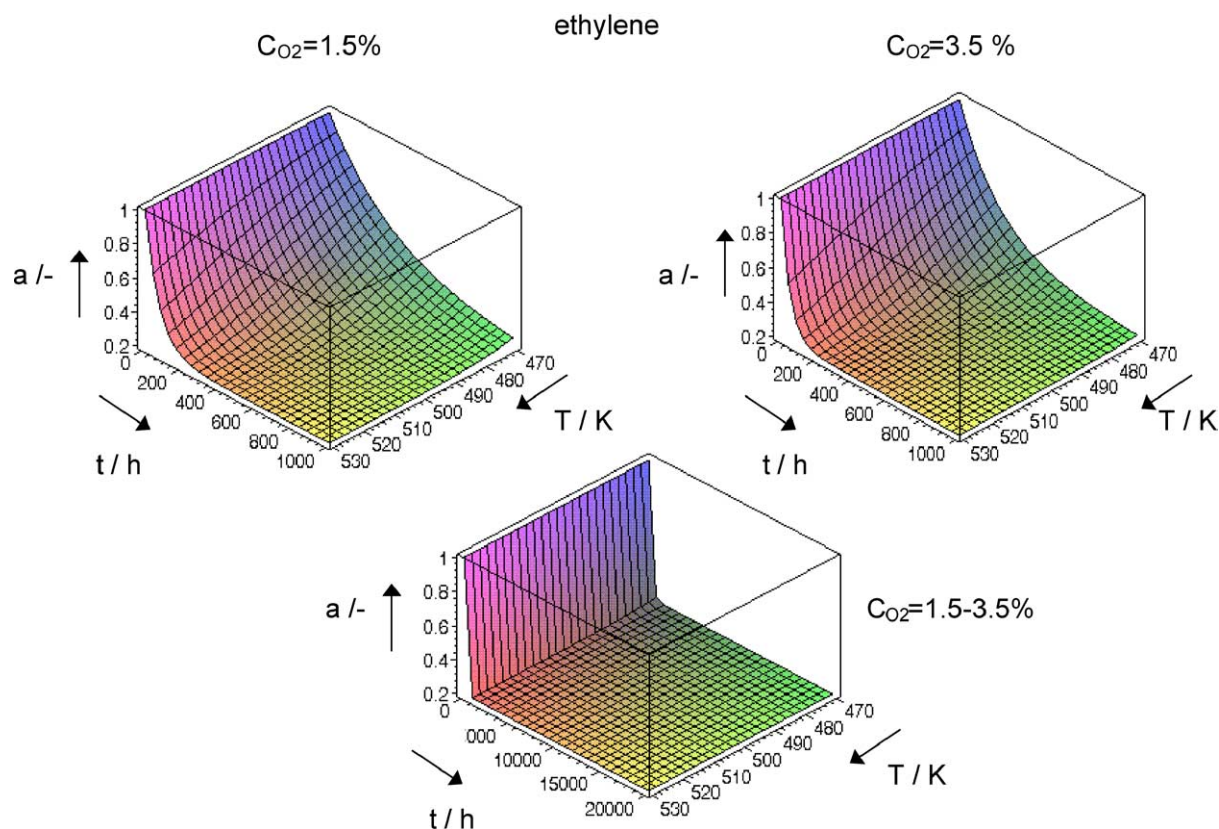


Fig. 12. The long-time prediction of catalyst activity of C_2H_4 for different concentrations of oxygen in a Bertly reactor, based on kinetic model given by Eq. (4).

For industrial applications, it would be highly desirable to develop catalysts that are more active at lower temperatures since raising the temperature in an industrial plant in order to keep the production of EO at a constant level simultaneously results in even faster deactivation, but more importantly also in lower selectivity.

The knowledge of kinetics of the catalytic reaction and deactivation is especially valuable since by knowing them in addition to the heat-transport process taking place in the industrial reactor, it is possible to solve the suitable reactor model and to predict the long-term performance of the reactor.

Notation

a	activity (–)
a_{ss}	steady-state activity (–)
C_{O_2}	volume percentage of oxygen (vol%)
d	order of deactivation with respect to driving force ($a - a_{ss}$) (–)
C_i	vol. fraction of component i (–)
p_{O_2}	partial pressure of oxygen (MPa)
R	reaction rate (mol/(L _{cat} h))
S	selectivity (%)
F_{tot}	total molar flow rate (mol/h)
V_{CAT}	catalyst volume (L)
α	exponent with respect to O_2 concentration (–)

Acknowledgments

Funding of this work by the European Commission Project GRD1-1999-10239 is highly appreciated. The authors also acknowledge the agreement of the industrial partners of the project to publish the work.

References

- [1] B. Delmon, *Appl. Catal.* 15 (1985) 1–17.
- [2] J.C. Zomerdijk, M.W. Hall, *Catal. Rev. Sci. Eng.* 23 (1981) 163–185.
- [3] S.B. Cavitt (Texaco Dev. Corp.) US 4097414, 1978; N. Rizkalla (Sci. Design. Co, Inc.) US 5374748, 1994; M. Metusz (Shell Oil Co) US 573907, 1998; E.W. Errol, C.P. Ingraham (Shell Oil Co) US 6717001, 2001.
- [4] J.C. Wu, P. Harriot, *J. Catal.* 39 (1975) 395–402.
- [5] X.E. Verykios, F.P. Stein, R.W. Coughlin, *J. Catal.* 66 (1980) 368–382.
- [6] G.B. Hoflund, J.F. Weaver, G.N. Salaita, D.M. Minahan, *Stud. Surf. Sci. Catal.* 126 (1999) 397–403.
- [7] G. Boxhoorn (Shell), EP207550A1 (1987), EP255975 (1988); L.A. Kapicak, A.W. Nauman, T.M. Noterman, E.M. Thorsteinsen (Union Carbide, Inc.) US4994588 (1989); N. Rizkalla (Scient. Design, Inc.) US5374748 (1994).
- [8] R. Christoph, M. Baerns, *Stud. Surf. Sci. Catal.* 34 (1987) 355–363.
- [9] N. Pernicone, *Appl. Catal.* 15 (1985) 17–31.
- [10] J.J. Birtill, *Stud. Surf. Sci. Catal.* 126 (1999) 43–62.
- [11] J.V. Porcelli, *Catal. Rev.-Sci. Eng.* 23 (1981) 151–162.
- [12] J.M. Oelderik, S.T. Sie, D. Bode, *Appl. Catal.* 47 (1989) 1–24.
- [13] P. Forzatti, L. Lietti, *Catal. Today* 52 (1999) 165–181.

- [14] J.A. Moulijn, A.E. van Diepen, F. Kapteijn, *Appl. Catal. A* 212 (2001) 3–16.
- [15] A.I. Kurilenko, N.V. Kulkova, L.P. Baranova, M.I. Temkin, *Kinet. Katal.* III 2 (1962) 208–213.
- [16] P.D. Klugherz, P. Harriot, *AIChE J.* 17 (4) (1971) 856–866.
- [17] S. Ghazali, D.W. Park, G. Gau, *Appl. Catal.* 6 (1983) 195–208.
- [18] L. Petrov, A. Elyas, D. Shopov, *Appl. Catal.* 24 (1986) 145–161.
- [19] R. Haul, G. Neubauer, *J. Catal.* 105 (1987) 39–54.
- [20] D.W. Park, G. Gau, *J. Catal.* 105 (1987) 81–94.
- [21] S.A. Tan, R.B. Grant, R.M. Lambert, *Appl. Catal.* 31 (1987) 159–177.
- [22] M.A. Al-Saleh, M.S. Al-Ahmadi, M.A. Shalabi, *Chem. Eng. J.* 37 (1988) 35–41.
- [23] J.T. Gleaves, A.G. Sault, R.J. Madix, J.R. Ebner, *J. Catal.* 121 (1990) 202–218.
- [24] E.P.S. Schouten, P.C. Borman, K.R. Westerterp, *Chem. Eng. Process.* 35 (1996) 107–120.
- [25] D. Lafarga, M.A. Al-Juaied, C.M. Bondy, A. Varma, *Ind. Eng. Chem. Res.* 39 (2000) 2148–2156.
- [26] T. Hattori, S. Komai, T. Hanaichi, A. Miyamoto, Y. Murakami, *Stud. Surf. Sci. Catal.* 34 (1987) 415–426.
- [27] E.P.S. Schouten, P.C. Borman, K.R. Westerterp, *Chem. Eng. Process.* 35 (1996) 43–55.
- [28] G. Boskovic, D. Wolf, A. Bruckner, M. Baerns, *J. Catal.* 224 (2004) 187–196.
- [29] O. Levenspiel, *J. Catal.* 25 (1972) 265–272.
- [30] J.B. Butt, E.E. Petersen, *Activation, Deactivation, and Poisoning of Catalysts*, Academic Press, New York, 1988.
- [31] J. Klose, M. Baerns, *J. Catal.* 85 (1984) 105–116.
- [32] A. Löwe, *Chem. Eng. Sci.* 37 (6) (1982) 944–945.
- [33] L.W. Jossens, E.E. Petersen, *J. Catal.* 73 (1982) 366–376.
- [34] A. Brückner, E. Kondratenko, H. Berndt, D. Muller, M. Baerns, *Proc. North Am. Catal. Soc., Toronto, 2001, Book of abstracts*.
- [35] C.H. Bartholomew, *Appl. Catal. A* 212 (2001) 17–60.
- [36] P.C. Borman, K.R. Westerterp, *Ind. Eng. Chem. Res.* 34 (1995) 49–58.
- [37] O. Levenspiel, *Omnibook*, Corvallis, Oregon, 1984.
- [38] I.E. Wachs, S.R. Kelemen, *J. Catal.* 71 (1981) 78–87.
- [39] I.E. Wachs, S.R. Kelemen, in: T. Seiyama, K. Tanabe (Eds.), *Proc. 7th ICC, New Horizons in Catalysis*, Elsevier, Tokyo, 1981, pp. 682–697.
- [40] M. Che, C.O. Bennett, *Adv. Catal.* 36 (1989) 55–172.
- [41] H.S. Fogler, *Elements of Chemical Reaction Engineering*, Prentice-Hall, Englewood Cliffs, NJ, 1968.
- [42] G.A. Fuentes, *Appl. Catal.* 15 (1985) 33–40.
- [43] G.A. Fuentes, E.D. Gamas, *Stud. Surf. Sci. Catal.* 68 (1991) 637–644.